Self-consistent electric field inside ordered dust structures

V. S. Vorob'ev, O. F. Petrov, and V. E. Fortov
Institute of High Energy Densities, Joint Institute of High Temperatures, Russian Academy of Sciences (IVTAN), Moscow, 125412 Russia
(Received 20 September 2007; published 6 March 2008)

We report finding a self-consistent electric field of electrons, ions, and dust grains inside an ordered dust cloud in glow discharge, and show that this field differs radically from that of an isolated grain. Besides, the screening radius coincides with the size of Wigner-Seitz cell. The value of potential necessary for containing dust particles in the direction perpendicular to the discharge axis is estimated. We show that the interaction potential energy of a system of ordered dust grains has a form characteristic of ionic crystals. Critical parameters for a liquidlike dust structure are estimated. The correlation function of dust grains obtained via this approach is compared with the measured function.

DOI: 10.1103/PhysRevE.77.036401 PACS number(s): 52.27.Lw, 52.27.Gr

I. INTRODUCTION

Gas-discharge dusty plasma is a partly ionized gas containing micron-sized dust grains with a high negative charge. Dust grains interact with one another and with plasma particles to form liquidlike or solidlike ordered structures [1,2]. Much attention is given in the literature to the search for effective pair potential describing the interaction between grains. It is further observed that, when ordinary multicomponent plasma of electrons and ions of different sorts is used to simulate dusty plasma, it is necessary to take into account a number of dusty plasma characteristic features [3–7]. One such characteristic feature is the dependence of the charge of grains on their concentration and on other parameters of the plasma. Another feature is the presence of permanent fluxes of plasma electrons and ions to grains, processes of surface recombination, and the need for permanent sources of ionization to sustain plasma existence. These sources are supported by energy input to the discharge. In particular, the presence of such fluxes results in a variation of the potential asymptotic at long distances [1–7]. At the same time, in spite of the abundance of dust plasma studies, the methods and approaches developed for ordinary multicomponent plasma are used too infrequently in application to this object. Regardless of the characteristic features mentioned above, a dust plasma system largely retains the features of multicomponent plasma. Charge grains and electrons and ions of plasma interact in accordance with the Coulomb law and are located in a self-consistent field generated by all charges.

In this paper the pair-correlation function of grains in glow discharge plasma is measured under the conditions when crystal- or liquidlike ordered dust structures were formed owing to the presence of some external "confinement" potential. Such structures have been observed over the last 15 years [1–7]. An adequate theoretical model is developed for interpretation of these observations and other experimental data. In the presence of the ordered dust structure, the solution of the Poisson-Boltzmann equation was obtained and a self-consistent potential was found. The latter potential is used to calculate the correlation function and potential energy of grains. It is demonstrated that the obtained result is in adequate agreement with the correlation function, measured here.

In the case when the ratio of mean distance between grains to ionic Debye radius is large (the screening of grains by plasma particles is strong), the potential energy of grains has a form characteristic of ionic crystals. When this ratio is small, the potential energy takes an ordinary Debye form, which is well known in plasma theory. The peculiar dependence of the charge of grains on their density leads to the emergence of a minimum in the density dependence of potential energy.

The contribution of potential energy to pressure is calculated, and it is demonstrated that the density dependence of potential energy has a minimum and two branches. Repulsive or attractive forces dominate the branches realized at high or low densities, respectively. The parameters of the critical point are estimated for a liquidlike dust structure.

II. BASIC PARAMETERS OF ORDERED DUST STRUCTURES IN GLOW DISCHARGE PLASMA

The formation of crystal-like or liquidlike dust structures was observed in the electrode layer of a radio-frequency (rf) capacitate discharge in argon. The pair (binary) correlation function given in Fig. 1 was specially measured for the purposes of the present study.

In brief, the experiment was performed in an rf discharge generated between two flat electrodes operating at a frequency of 13.56 Mhz, and a glow discharge was ignited between the electrodes in the argon atmosphere. During the experiment, the vacuum chamber was filled with argon at pressure $P_g \sim 1$ mBar. Grains were injected into the plasma from a special container via an opening in the upper electrode. The macroparticles used were either plastic spheres 1.9 μm in diameter or polydisperse particles (Al_2O_3) 2–5 μm in diameter. In the discharge, the grains were charged negatively and levitated in a sheath region above the lower electrode, where the electric field was strong enough to balance the gravity.

The video record of the experiment was processed using custom software which enabled one to identify the positions of individual particles in the field of view of the video system and to construct a binary correlation function (CF) for each dust-plasma structure obtained. It should be mentioned that this dust formation was about 5 cm in diameter, about

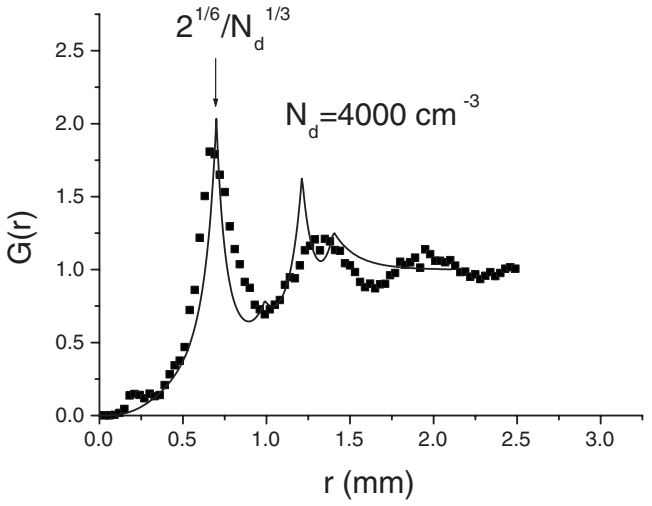

FIG. 1. Symbols correspond to the correlation function measured in this paper (N_d=4000 cm^{-3}). Solid line is the calculation according to Eq. (37).

1 cm in height, and had a very uniform structure because of the intensive thermal motion. These facts allowed us to consider this dusty plasma system to be a uniform three-dimensional (3D) structure. The CF in Fig. 1 is given for the dust component density N_d=4000 cm^{-3}. Its form is typical of the ordered state of matter. For example, the first maximum of CF in Fig. 1 corresponds to the first maximum of CF of face-centered crystal determined from the relation

$$R = 2^{1/6}/N_d^{1/3} \approx 0.7 \text{ mm}. \tag{1}$$

This allows one to assume that each grain is surrounded by a sphere of radius R on the surface of which 12 nearest neighbors are located. Assuming that the dust crystal is ideal, this must be followed by a sphere with six second neighbors at distance $R_1=R\sqrt{2}$, the third sphere with 24 particles at distance $R_2=R\sqrt{3}$, and so on. The position of particles is localized in space, and they are capable only of performing vibrations in the vicinity of equilibrium positions. The electrons and ions of glow discharge plasma move between dust particles to provide for their charging and screening. The plasma parameters typical of glow discharge are as follows: the ion concentration $N_i \approx 10^8$ cm^{-3}, the ion temperature $T_i \sim 0.05$ eV, and the electron temperature $T_e \sim 2$ eV. In these conditions, the screening radius is defined by ions and its value is $R_i=\sqrt{T_i/4\pi e^2 N_i} \approx 0.17$ mm. The ratio $R/R_i \approx 4.2$ indicates that the ionic Debye radius is much shorter than the mean distance between dust particles and, therefore, the screening of grains by plasma charges is significant.

Here we consider the following relation between different typical lengths:

$$a \ll R_i < R \ll \lambda_{i(e)}, \tag{2}$$

where $\lambda_{i(e)}$ is the ion (electron) mean free path. In this approach ions and electrons move without collisions except at the grain surface, where absorption takes place. If the inequality $\lambda_{i(e)} < R_i < R$ is valid, then both electron and ion transport to the grain is collision dominated. Such a case has been recently investigated in Refs. [8,9]. Under the experimental conditions considered above, ion transport may be partially collision driven ($R \sim \lambda_i$), and electron transport to the grain is collisionless. In this paper, in the first approximation we will neglect ion-neutral collision and consider fully collisionless transport both for electrons and ions. The collision-dominated regime in ordered dusty system calls for further investigations.

For ensuring the levitation of dust particles in the experiment, it is further necessary that the force of gravity would balance the electric force, i.e.,

$$M_d g = ZeE, \tag{3}$$

where M_d is the grain mass, and E is the component of electric field strength which is directed along the discharge axis. Therefore, if the field intensity does not vary, a certain concentration of dust particles reaches a steady-state value in the discharge.

We assume that the dust particle radius is $a=5$ μm and derive $Z \approx 10\,000-15\,000$. The quantity $ZN_d \approx 4\times 10^7$ cm^{-3} makes up for a sizable fraction of the electron concentration. We find from the condition of electroneutrality

$$N_i = N_e + ZN_d \tag{4}$$

that $N_e \approx 6\times 10^7$ cm^{-3}, which is much lower than the value of ion concentration. Here N_e, N_i, and N_d are concentrations of electrons, ions, and grains averaged over the dusty cloud.

Note further that, despite the relatively high temperature of translational motion of ~ 5 eV, the velocity of thermal motion of grains remains very low (~ 1 cm/s or less) because of the large mass ($M_d \sim 5\times 10^{-10}$ g). Therefore, grains are stationary sources of charge losses with respect to thermal motion of plasma electrons and ions.

III. MODEL OF ORDERED STRUCTURES OF DUST GRAINS

The problem is formulated as follows. We consider a small individual charged grain immersed in isotropic plasma and surrounded by spherical layers containing other grains. Every layer is at a distance $R_i=R\sqrt{i}$ from the central grain and contains m_i dusty grains whose charge is uniformly distributed on a spherical surface of radius R_i. The central grain forms a nonuniformly charged cloud (spherical symmetric on the average) around itself. This cloud is characterized by a self-consistent potential Φ.

Let us assume that grains form a structure similar to that of face-centered crystal ("dust crystal"). In this case, a layer of 12 nearest neighbors surrounds the initially selected grain of charge Z. Then this is followed by the second layer formed by six particles at distance $R\sqrt{2}$, the third layer of 24 particles at distance $R\sqrt{3}$, and so on. Table I gives the distances from the origin particle $r_i=R\sqrt{i}$ and the respective coordination numbers for the face-centered crystal.

If the dust particles form a liquidlike structure ("dust liquid"), the number of nearest neighbors in the layers becomes somewhat smaller than that for ideal crystal because of the formation of vacancies and other structural defects. Accord-

TABLE I. The distances from the origin particle $r_i=R\sqrt{i}$ and the respective coordination numbers for the face-centered crystal.

Number of layer, i	1	2	3	4	5	6	7	8	9	10	11	12	13
Distance, r_i	1	$\sqrt{2}$	$\sqrt{3}$	$\sqrt{4}$	$\sqrt{5}$	$\sqrt{6}$	$\sqrt{7}$	$\sqrt{8}$	$\sqrt{9}$	$\sqrt{10}$	$\sqrt{11}$	$\sqrt{12}$	$\sqrt{13}$
Crystal, m_i	12	6	24	12	24	8	48	6	36	24	24	24	72
Liquid, m_i	10.5	5.5	22	—	—	—	—	—	—	—	—	—	—

ing to the data of Ref. [10], this number in the first coordination sphere is 10.5 instead of 12, in the second coordination sphere is ~5.5, and in the third sphere is 22. Table I gives coordination numbers for the liquid state for the first three coordination spheres. In the case of long distances, the layers are mixed because of the thermal motion and the so-called structural diffusion [11], the order is lost, and the dust particles are distributed uniformly. In this case, the number of particles in the spherical layer from $R\sqrt{i}$ until $R\sqrt{i}$ to $R\sqrt{i+1}$ is determined as

$$m_i = 4\pi R^3 i(\sqrt{i+1}-\sqrt{i})N_d \approx 2\pi\sqrt{2i}. \tag{5}$$

We follow Frenkel [11] and represent the dust particle distribution function as

$$\rho(r) = \frac{1}{4\pi r^2}\sum_i g_i(r). \tag{6}$$

For an ideal crystal, the sum of δ functions $g_i(r)=m_i\delta(r-r_i)$ is under the summation sign in Eq. (6). In the general case, the function introduced above may be determined as the sum of a series of Gaussian functions

$$g_i(r) = \frac{m_i}{\sqrt{2\pi D}}\exp\left(-\frac{(r-r_i)^2}{2D}\right). \tag{7}$$

The dispersion $D=D_T+D_S$ characterizes the mean-square deviations of particles from the equilibrium position, which occur due to thermal motion (D_T) and structure defects (D_S). We write the part of dispersion associated with thermal motion as $D_T=T/k$, where k is the coefficient of rigidity. The structure defect part of dispersion D_S is connected with an increase of statistical scattering of particle position distribution due to the lack of long order for liquid. This value increases proportionally to the square root of the mean distance of the respective layer from the central grain, i.e., $D_S=2Sr_i$, where S is some constant which has the dimension of length.

As r increases, the spacing between neighboring layers become narrower and the width of the layers increases; therefore, a permanent "background" of $\rho=N_d$ is finally formed that corresponds to the average concentration of dust particles. Below we will use Eq. (6) with the δ function for the first and several following layers; for the subsequent layers, we will assume the distribution to be uniform.

IV. CHARGING OF GRAINS

In our approach, ions and electrons are assumed to move without collisions, except at the grain surface where absorption takes place. Since the average distance between the grains is sufficiently large in the sense that other dusty grains do not affect the motion of electrons and ions in the vicinity of a separate grain, the orbit motion limited (OML) approximation with Havnes parameter [1,2] is applicable. The charge of grains Z and electron (I_e) and ion (I_i) fluxes to the particle surface can be estimates from the expressions

$$I_i = \sqrt{8\pi}a^2N_i\sqrt{\frac{T_i}{M}}\left(1+\frac{e^2Z}{T_ia}\right),$$

$$I_e = \sqrt{8\pi}a^2N_i\left(1-\frac{ZN_d}{N_i}\right)\sqrt{\frac{T_e}{m}}\exp\left(-\frac{Ze^2}{T_ea}\right),$$

$$I_i = I_e = I, \tag{8}$$

where Z is the absolute value of the grain charge and a is the grain radius, m and M denote the mass of electron and ion, respectively. From Eq. (8), one can readily obtain the correlation between the density of grains and their charge

$$N_d = \frac{N_i}{Z}\left[1-e^{Ze^2/aT_e}\left(\frac{mT_i}{MT_e}\right)^{1/2}\left(1+\frac{Ze^2}{aT_i}\right)\right] \tag{9}$$

The charge of grains decreases with increasing grain concentration. For fixed values of T_e, T_i, M, Z, and a, the dust concentration is proportional to the ion concentration. If the ion density does not vary, a variation of the density of dust particles is accompanied by a variation of their charge.

V. DISTRIBUTION OF CHARGE PARTICLES AND SELF-CONSISTENT FIELD AROUND A GRAIN

We consider the density distribution of electrons $n_e(r)$ and ions $n_i(r)$ relative to the initially selected grain at the origin surrounded by spherical layers. Every grain acts as a plasma sink by absorbing ions and electrons. This implies that plasma compensation occurs far from the grain, i.e., the characteristic ionization (recombination) length is considerably larger than the length scale under consideration. Within these assumptions, the dusty grain absorbs ion and electron fluxes. In this approach, ion density distribution is described by the expressions calculated in Ref. [12],

$$n_i(r) = N_i\left\{\frac{2}{\sqrt{\pi}}\sqrt{-\Phi/T_i}+\exp(-\Phi/T_i)\right.$$
$$\left.\times[1-\mathrm{erf}(\sqrt{-\Phi/T_i})]\right\} \quad \text{for } r \gg a,$$

$$n_i(r) = \frac{N_i}{2}\left\{ \frac{2}{\sqrt{\pi}}\sqrt{-\Phi/T_i} + \exp(-\Phi/T_i) \times [1 - \mathrm{erf}(\sqrt{-\Phi/T_i})] \right\} \quad \text{for } r \to a, \tag{10}$$

where $\mathrm{erf}(x)$ is the probability integral and Φ is the self-consistent potential. Note that the electron distribution tends to a Boltzman distribution. Expressions (10) are supplemented by the Poisson equation

$$\frac{1}{r^2}\frac{d}{dr}\left(r^2\frac{d\Phi}{dr}\right) = -4\pi e[n_e(r) - n_i(r) - Z\rho(r)], \tag{11}$$

where

$$\rho(r) = \sum_s \frac{m_s \delta(r - R_s)}{4\pi r^2}$$

for small r and $\rho = N_d$ for large r.

It is useful to introduce dimensionless variables $x = r/R$, $z = Ze^2/RT_i$, $\varphi = e\Phi/zT_i$, and the following shorthand notations: $\delta = N_e/N_i$, $\tau = T_i/T_e$, and $\alpha = R/R_i$. We rewrite Eq. (11) with the following dimensionless variables and notations:

$$\varphi'' + \frac{2}{x}\varphi' = \frac{\alpha^2}{z}[\Psi(z\varphi) - \delta e^{-\tau z\varphi}], \tag{12}$$

where $\psi(t) = \psi_1(t)$ if $r \gg a$ and $\psi(t) = \psi_1(t)/2$ if $r \to a$. The function $\Psi_1(t)$ is determined as

$$\Psi_1(t) = \frac{2\sqrt{\varphi(t)}}{\sqrt{\pi}} + e^{\varphi}\{1 - \mathrm{erf}[\sqrt{\varphi(t)}]\}.$$

In a linear approximation with respect to φ ($e^{\varphi} \approx 1 + \varphi$), Eq. (12) has the form

$$\varphi'' + \frac{2}{x}\varphi' - \alpha^2(1 + \delta\tau)\varphi = \alpha^2\frac{1 - \delta}{z} \quad \text{for } r \gg a \tag{13}$$

and

$$\varphi'' + \frac{2}{x}\varphi' - \alpha^2(1/2 + \delta\tau)\varphi = \alpha^2\frac{1/2 - \delta}{z} \quad \text{for } r \to a. \tag{14}$$

The quantity $\delta\tau$ accounts for the importance of electrons in regards to screening in nonisothermal plasma. Under the conditions of glow discharge, this quantity is small and we will neglect it in the following considerations.

VI. SOLUTION OF THE POISSON EQUATION

Let us first find the solution for the case where a dust particle of charge Z is surrounded by concentric spheres of radii $R\sqrt{i}$, on which the charge Zm_i is distributed uniformly. Plasma electrons and ions move freely between these spheres. "Jumps" of charges by Zm_i arise on the layer boundaries.

Because the particle radius is small ($a \ll R$), the boundary condition at $r \to 0$ has the form

$$\Phi(r)|_{r\to 0} = -\frac{Ze}{r}. \tag{15}$$

In dimensionless variables, Eq. (15) is simplified and takes the form

$$\varphi(x)|_{x\to 0} = \frac{1}{x}. \tag{16}$$

The solution of Eqs. (13) and (14) may be represented as

$$\varphi = \varphi_c + \omega, \tag{17}$$

where φ_c and ω denote the constant and variable components of potential, respectively. The constant component arises because of a violation of the charge symmetry caused by the presence of an appreciable amount of dust grains, $N_e < N_i$, and Eq. (13) permits a solution $\varphi_c = \mathrm{const}$ and

$$\varphi_c = -\frac{1 - \delta}{z} = -\frac{4\pi\sqrt{2}}{\alpha^2}. \tag{18}$$

When Eqs. (3) are used, the respective dimensional potential has the form

$$\Phi_c = -\frac{T_i Z N_d}{eN_i} = -\frac{T_i}{e}\left[1 - e^{Ze^2/aT_e}\left(\frac{mT_i}{MT_e}\right)^{1/2}\left(1 + \frac{Ze^2}{aT_i}\right)\right]. \tag{19}$$

Hence it follows that the constant component of the self-consistent potential does not exceed the ion temperature. It is zero for an isolated grain and approaches a value of $-T_i/e$ with an increase in the concentration of grains and a decrease in their charge.

Equation (14) is valid near the grain, and its solution when $\delta \sim 1$ has the form $\varphi \approx 1/x + 1/z$, while the solution of Eq. (13) is $-1/x - (1/\delta)/z$. Near the grain, the value $1/x \sim R/a \gg 1$, whereas the values of $1/z$ and $(1-\delta)/z$ are restricted. So, the difference between these solutions can be neglected. Below we will construct a solution of Eq. (13).

We will now find the variable component. The peculiarity of the problem lies in the presence of spherical layers, in which a jump of the charge occurs. In so doing, the potential must remain continuous.

We will consider the first layer $0 \leqslant x \leqslant 1$. The solution for the potential will be sought in the form

$$\omega_0(x) = \frac{1}{x}(Ae^{\alpha x} + Be^{-\alpha x}). \tag{20}$$

The constant B is found from the condition that the potential must follow the Coulomb form at $x \to 0$, i.e., $\omega(x) \to 1/x$. Hence it directly follows that

$$B = 1 - A. \tag{21}$$

The charge corresponding to Eq. (20) is found from the relation

$$z_0(x) = -r^2\frac{d\omega_0}{dx} = -Ae^{\alpha x}(\alpha x - 1) + Be^{-\alpha x}(\alpha x + 1). \tag{22}$$

In the next layer $1 \leqslant x \leqslant \sqrt{2}$, we will seek the solution in the form

$$\omega_1(x) = A_1 e^{\alpha x} + B_1 e^{-\alpha x}, \tag{23}$$

$$z_1(x) = -A_1 e^{\alpha x}(\alpha x - 1) + B_1 e^{-\alpha x}(\alpha x + 1). \tag{24}$$

The boundary conditions have the form

$$\omega_0(1) = \omega_1(1), \quad z_0(1) + m_1 = z_1(1), \tag{25}$$

where m_1 is the charge jump during the passage through a layer.

From conditions (30) and (32)–(34), we find that

$$A_1 = A - \frac{n_1 e^{-\alpha}}{2\alpha}, \tag{26}$$

$$B_1 = B + \frac{n_1 e^{\alpha}}{2\alpha}. \tag{27}$$

The solutions for the subsequent layers are constructed similarly. One can readily demonstrate that the coefficients A_i and B_i, which define the solution in the ith layer, are related to the coefficients A_{i-1} and B_{i-1} by the recursive formula

$$A_i = A_{i-1} - \frac{n_i e^{-\alpha\sqrt{i}}}{2\alpha\sqrt{i}}, \tag{28}$$

$$B_i = B_{i-1} + \frac{n_i e^{\alpha\sqrt{i}}}{2\alpha\sqrt{i}}. \tag{29}$$

Equations (26) and (27) yield

$$A_n = A - F_n^-, \tag{30}$$

$$B_n = 1 - A + F_n^+, \tag{31}$$

where

$$F_n^- = \frac{1}{2\alpha}\sum_{i=1}^{n} \frac{n_i e^{-\alpha\sqrt{i}}}{\sqrt{i}}, \quad F_n^+ = \frac{1}{2\alpha}\sum_{i=1}^{n} \frac{n_i e^{\alpha\sqrt{i}}}{\sqrt{i}}. \tag{32}$$

We will further assume that, at $x \geqslant \sqrt{N}$, the particles are distributed uniformly. In this case, a constant term ZN_d appears on the right-hand side of Eq. (11), and the left-hand side of Eq. (13) must be zero. The solution has the Debye form

$$\tilde{\omega} = C_N e^{-\alpha x}/x. \tag{33}$$

The constant C_N is found from the condition $\tilde{\omega}(\sqrt{N}) = \omega_N(\sqrt{N})$, which leads to the value

$$C_N = A_N e^{2\alpha\sqrt{N}} + B_N - 4\pi\sqrt{2N} e^{\alpha\sqrt{N}}/\alpha^2. \tag{34}$$

The procedure for the calculation of the constant A will be described below.

Figures 2(a), 2(b), 3(a), and 3(b) give (a) the potential $\varphi(x)$ and (b) the charge $z(x)$ as functions of distance x for three values of the parameter α [Fig. 2(a)]. In Figs. 2(a) and 2(b), the charge jumps in the first nine layers were taken in accordance with Table I, i.e., as in the case of the ideal crystal. It was further assumed that the charge was distributed uniformly. The charge jumps in Figs. 3(a) and 3(b) were taken into account in the first four layers in accordance with Table I for the liquid. The lines in Figs. 2(a) and 3(a) correspond to (1) $\alpha=8$, (2) 4.25, and (3) 2.

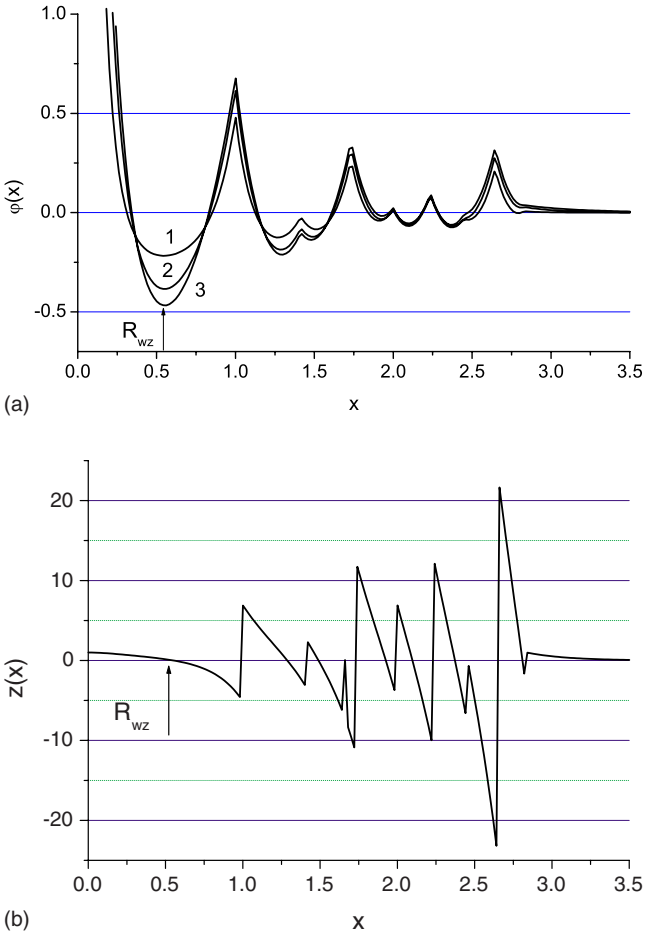

FIG. 2. (Color online) The dependence of the potential (a) $\varphi(x)=\omega(x)-4\pi\sqrt{2}/\alpha^2$ and charge (b) on the dimensionless distance x for the crystal-like structure, following from the solution of Poisson-Boltzman equation when nine layers of dust particles are taken into account. The values of m_i for the first nine layers were taken from Table I for solid state and for consequent layers were calculated according to Eq. (6). Line 1 in Fig. 1(a) corresponds to the value of $\alpha=8$, 2–4.25, 3–2.5.

In both cases, the potential derivative experiences a discontinuity at the boundary between layers, which is associated with the charge jump at this boundary. This discontinuity is the consequence of the assumption regarding "jumps" of charges arising on the layer boundaries. The potential derivative will be smoother if we take into account the discreteness of the charges distributed on a spherical surface.

Upon transition to uniform distribution, these kinks cease, and the potential approaches zero smoothly. With the proviso that $\alpha \geqslant 1$, the distribution of potential φ between layers depends rather weakly on the parameter α. The charge distribution is almost independent of the parameter α; therefore, Figs. 2(b) and 3(b) show a graph only for $\alpha=4.25$. The graph begins with the value of $z=1$, which corresponds to the dimensionless charge of the particle at the origin. As x increases, this charge is screened by plasma ions and changes sign to negative. At point $x=1$, the charge jumps by 12. Then

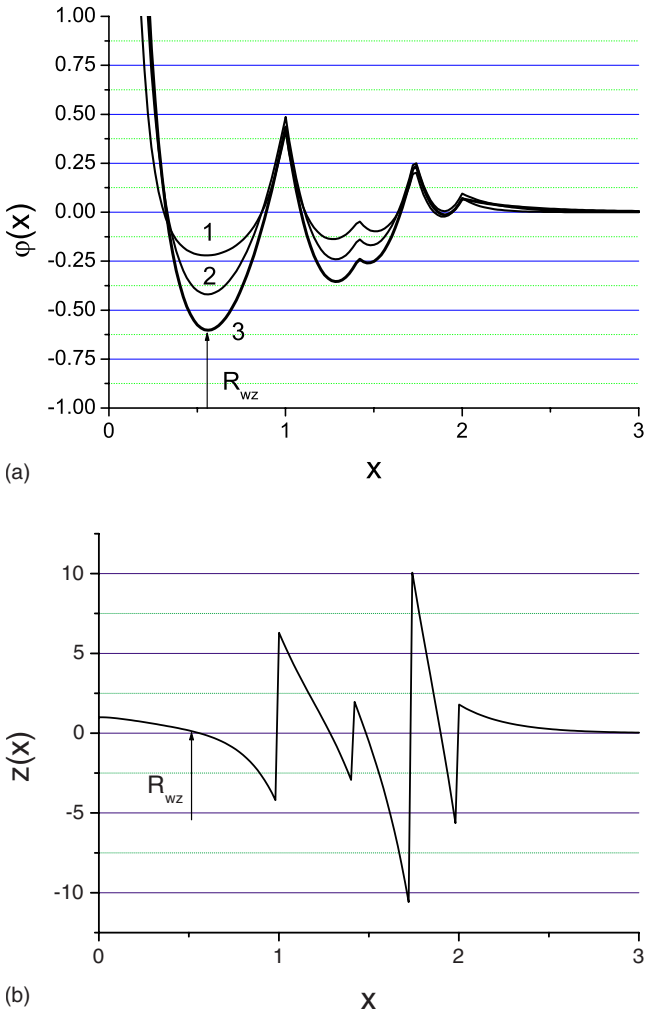

FIG. 3. (Color online) The same as Fig. 2 for liquidlike structure. The values of m_i for first three layers were taken from Table I for liquid state and for consequent layers were calculated according to Eq. (6).

the pattern repeats, and at point $x=\sqrt{2}$ the charge increases by six, and so on. When the distribution becomes uniform, the jumps cease, and the charge decreases smoothly.

We can see that the potential φ in the space between the grain and first layer of the nearest neighbors changes sign and reaches a minimum (maximum with regard to the grain charge). Its value with regard to the grain sign at the point of the maximum is positive and equal to about 0.5. As it follows from Fig. 2, the deviation from the Boltzman law is not great yet at such positive values of the self-consistent potential.

VII. CONFINEMENT POTENTIAL

Note that the distance at which the charge is fully screened for the first time, and the potential has a minimum, coincides with the size of Wigner-Seitz cell $R_{\mathrm{WZ}}=(3/4\pi)^{1/3}(1/N_d^{1/3})=0.62/N_d^{1/3}$. Figure 4 gives the value of potential at the cell boundary $\varphi(R_{\mathrm{WZ}})$ as a function of parameter α. Also given in this figure is the potential $-\varphi_c$ (dashed line). At $\alpha \leqslant 1$, the potential $\varphi(R_{\mathrm{WZ}}) \approx -\varphi_c$. In the case of

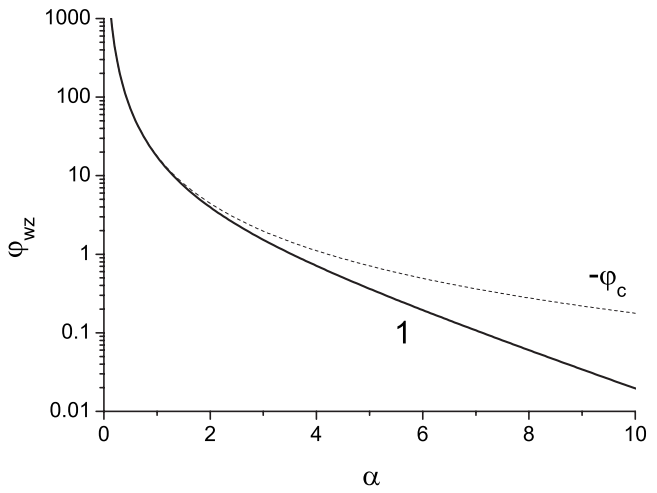

FIG. 4. The dependence of the potential on the boundary of Wigner-Seitz cell on the parameter α (line 1); the dotted line is the potential $-\varphi_c$.

high values of, the inequality $\varphi(R_{\mathrm{WZ}}) \approx -\varphi_c$ is valid.

We will treat a dust system as a set of Wigner-Seitz cells. In this case, the boundary layer of such a system must consist of positive ions. For these ions not to be displaced, the entire system must be located in a potential trap formed by negative charges. The trap potential φ_s must exceed in magnitude at least the potential on the boundary of the Wigner-Seitz cell, i.e., $\varphi_s \geqslant \varphi_{\mathrm{WZ}}$. One can further use the theory of restricted orbital motion to estimate the wall potential, if Ze/a in the formulas of this theory is formally replaced by φ_s, where φ_s is the wall potential. Then Eq. (12) yields, within a geometric factor on the order of unity, the condition of confinement of dust plasma in the form

$$e\varphi_s \sim Ze^2/a \geqslant \Phi_{\mathrm{WZ}}. \tag{35}$$

Figure 5 gives a qualitative pattern of distribution of potentials at the wall which bounds the volume with dust plasma. Inequality (35) may be rewritten as

$$\frac{R}{R_i} > \left(\frac{4\pi\sqrt{2}aT_i}{Ze^2}\right)^{1/2}. \tag{36}$$

For the plasma parameters under consideration, this is equivalent to $R/R_i > 1$. Therefore, for the confinement of dust plasma, it is required that the mean distance between

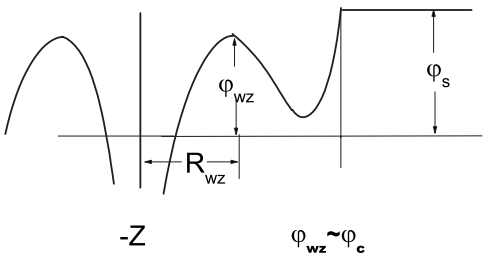

FIG. 5. The qualitative picture of the potential distribution near the dusty boundary: φ_s is the wall potential, φ_{WZ} is the potential on the boundary of Wigner-Seitz cell.

dust particles would exceed the ionic Debye radius, i.e., the screening of dust charges by plasma charges must be significant.

VIII. CORRELATION FUNCTION

In the approximation under consideration, dust particles interact directly with plasma electrons and ions. As to the interaction of dust particles with one another, it may be reduced to the effect of some self-consistent field on each one of these particles. This field is, on the average, isotropic, i.e., it exhibits spherical symmetry. To find this field, we subtract the potential of the central dust particle in consideration of screening from the self-consistent potential found above, i.e., we will consider the quantity

$$e\tilde{\Phi}(r) = e\Phi(r) - e^2 Z e^{-r/R_r}(1 + r/R_i)/r. \tag{37}$$

In the case of low values of r, the potential $\tilde{\Phi}(r) \to -\Phi_c$ and becomes negative. It oscillates with increasing r and, in the case of high values of r, asymptotes to zero. The probability of finding a dust particle at a distance r from the origin of coordinates, i.e., the correlation function, may be written as

$$G(r) = \exp[-e\tilde{\Phi}(r)/T_i r]. \tag{38}$$

The ion temperature is used in Eq. (38) because it is the main component which forms the self-consistent field, and the dynamics of screening of dust particles are defined by the velocity of motion of ions. We make a transition to dimensionless variables and can rewrite Eq. (46) as

$$G(x,\alpha,z) = \exp\{z\alpha[\varphi(x,\alpha) - e^{-\alpha x}(1 + \alpha x)/x]\}. \tag{39}$$

This correlation function depends, in addition to distance, on two dimensionless parameters α and z. The function for liquidlike dust structure, calculated by Eq. (39), is shown in Fig. 1 as a continuous line. The following values of parameters are used: $Z=10\,000$, $T_i=0.05$ eV, $R_i=0.017$ cm, and $R=0.074$ cm. The calculated function reproduces the first maximum of the experimentally obtained function fairly well. The subsequent maxima of the calculated correlation function are located at somewhat shorter distances than the measured ones. This is indicative of the difference between the experimentally realized real dust structure and the assumed structure used in the calculation. Qualitatively, the calculation results reproduce all of the characteristic features of the measured correlation function quite adequately. In addition, the method under consideration allows varying the coordination numbers and distances between layers for better agreement with the experimental data.

Formula (39) yields the expression for the first maximum of the correlation function, which may be conveniently written as

$$\ln G_m = \frac{Ze^2}{T_i R_i}\chi(\alpha), \tag{40}$$

where

$$\chi(\alpha) = A(e^{\alpha} - e^{-\alpha}) - \frac{4\pi\sqrt{2}}{\alpha^2} - \alpha e^{-\alpha}. \tag{41}$$

In the $3 < \alpha < 9$ range, the function $\chi(\alpha)$ varies only slightly and is $\chi(\alpha) \approx 0.41$. This enables one to find the charge of dust particles from Eq. (40) from the value of correlation function in the first maximum. It follows from the experimental graph of Fig. 1 that $\ln G_m \approx 0.64$. We assume that $T_i=0.05$ eV and $R_i=0.017$ cm to obtain $Z \approx 92000$. This value agrees rather well with that obtained using the theory of restricted orbital motion ($Z \approx 98000$).

IX. INTERACTION ENERGY

We follow [13] and present the energy of interaction of dust particle with electrons and ions per unit volume in the form

$$U = 2\pi N_d \int_0^{\infty} r^2 dr[N_{e0} V_{de} G_{de} + N_{i0} V_{di} G_{di}], \tag{42}$$

where $V_{de}=Ze^2/r$ and $V_{di}=-Ze^2/r$ are the potentials of interaction of dust particle with electron and ion, respectively. In Eq. (42), G_{de} and G_{di} are the respective correlation functions which have the form

$$G_{de} = \exp\left(\frac{e\Phi}{T_e}\right) - 1, \quad G_{di} = \exp\left(\frac{-e\Phi}{T_i}\right) - 1. \tag{43}$$

We substitute Eq. (43) into Eq. (42) and make a transition to dimensionless variables in the linear (with respect to Φ) approximation to derive

$$U = -\frac{2\pi e^4 Z^2 N_d N_{io} R}{T_i} u(R/R_i), \tag{44}$$

$$u = \int_0^{\infty} \varphi(1 + \delta\tau) x dx \cong \int_0^{\infty} (\omega + \varphi_c) x dx. \tag{45}$$

If we assume in Eq. (42) that $N_d=N_i$ and $Z=1$, and use the Debye approximation $\varphi=\exp(-\kappa r)/r$ for the correlation addition, where κ is the inverse Debye radius, we obtain the well-known negative Debye addition to the energy of electron or ion. The negative sign of this addition is associated with the fact that unlike charges in plasma are, on average, located closer to one another than like charges.

For the problem under consideration, integral (45) is calculated analytically. For this purpose, we substitute ω into Eq. (45) in the form $\omega=(1/\alpha^2)[\omega''+(2/x)\omega']$; this form follows from the Poisson equation for this function. After integration, we derive

$$u(\alpha) = \frac{1}{\alpha^2}[(x\omega' + \omega)|_0^{\sqrt{N}} - 2\pi\sqrt{2N} + \alpha C_N e^{-\alpha\sqrt{N}}]. \tag{46}$$

We use the fact that $x\omega' = z(x)/x$. The latter function has a discontinuity of the first kind during transition through each layer. The value of this discontinuity upon transition through the ith layer is found from the condition

$$-\left.\frac{z(x)}{x}\right|_{x\to\sqrt{i}-0}+\left.\frac{z(x)}{x}\right|_{x\to\sqrt{i}+0}=\frac{n_i}{\sqrt{i}}. \tag{47}$$

As a result, the interaction energy may be written as

$$u(\alpha)=\frac{1}{\alpha^2}\left[\sum_{i=1}^{N}\left(\frac{n_i}{\sqrt{i}}-2\pi\sqrt{2}\right)+\frac{d}{dx}(x\omega)\Big|_{x\to 0}^{\sqrt{N+1}}+\alpha C_N e^{-\alpha\sqrt{N}}\right]. \tag{48}$$

The quantity

$$\frac{d}{dx}(x\omega)\Big|_{x\to 0}^{\sqrt{N}}+\alpha C_N e^{-\alpha\sqrt{N}}=\alpha T(\alpha,N) \tag{49}$$

may be represented in the form where

$$T(\alpha,N)=1+2A(e^{\alpha\sqrt{N}}-1)-2e^{\alpha\sqrt{N}}\Sigma_N^-+4\pi\sqrt{2N}/\alpha^2. \tag{50}$$

If the dust particles are distributed uniformly, the sum in Eq. (48) goes to zero. The dust particle at the origin is screened by plasma particles, and the relation $u(\alpha)=1/\alpha$ leading to an ordinary Debye correction to the particle energy must be valid. Therefore, it is necessary to demand that the function $T(\alpha,N)=1$. In addition, the result in this case will be independent of N. We select the constant A so that this condition would be valid. Equation (50) gives

$$A=\frac{2\pi\sqrt{2N}/\alpha^2+e^{\alpha\sqrt{N}}\Sigma_N^-}{e^{\alpha\sqrt{N}}-1}. \tag{51}$$

At $\alpha\ll 1$, $A\approx 2\pi\sqrt{2}/\alpha^3$; when the parameter $\alpha>1$, $A\approx F_N^-$. The interaction energy given by Eq. (44) assumes the form typical of ionic crystals [14,15],

$$U=-\frac{e^2Z^2(N_d)^2N_d^{4/3}}{2\times 2^{1/6}}M, \tag{52}$$

where

$$M=\alpha+\mu, \tag{53}$$

$$\mu=\sum_{i=1}^{N}\left(\frac{n_i}{\sqrt{i}}-2\pi\sqrt{2}\right) \tag{54}$$

is the effective Madelung parameter.

If the value of parameter α is high, the first term in Eq. (53) is dominant, and ordinary Debye screening of the central dust particle by plasma occurs. In the case of a moderate value of the parameter α, the second term in Eq. (53) becomes the principal term. Then the energy of the interaction of the dust particles (52) has the form of Madelung energy, i.e., the same as that for a highly correlated classical ionic system. Function (53) is an analog of the Madelung constant for a highly correlated system of charged dust particles. For the emergence of this function, it is necessary that $n_i/\sqrt{i}\neq 2\pi\sqrt{2}$.

We perform the calculation for crystal-like and liquidlike dust structures. In the former case, we assume that the charges n_i for the first nine layers are distributed as in a crystal and, starting with the tenth layer, $n_i/\sqrt{i}\approx 2\pi\sqrt{2}$. Then, $\mu=\Sigma_{i=1}^{9}\left(\frac{n_i}{\sqrt{i}}-2\pi\sqrt{2}\right)=2.39$. This value is close to that of the Madelung constant for the lattice of sodium chloride equal to 1.747 [15]. The respective quantity $u(\alpha)$ is $u(\alpha)=(2.39+\alpha)/\alpha^2$.

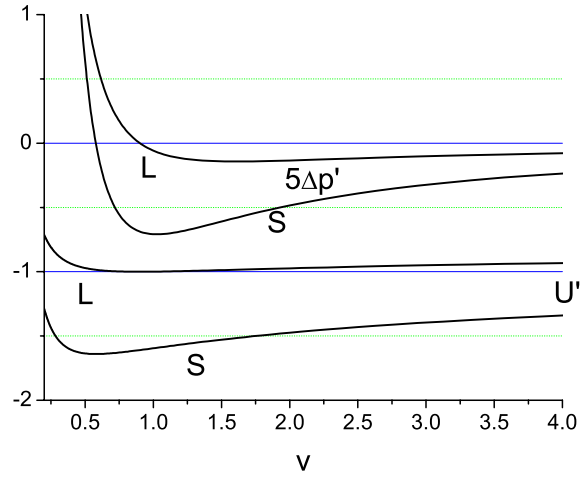

FIG. 6. (Color online) Two lower lines are the dependencies of the reduced potentials $U'=U/U_mN_d$ on the reduced specific volume $v=N_m/N_d$ for liquid (L) and crystal (S), respectively. The values are $U_m=510$ eV and $N_m=1000$ cm^{-3}. Two upper lines are the same for the potential contribution for the pressure $\Delta p'=\Delta p/U_mN_m$.

In the latter case, we assume that the charges Z_i for the first three layers are distributed as in a liquid (see Table I) and, starting with the fourth layer, $n_i/\sqrt{i}\approx 2\pi\sqrt{2}$. The quantities μ and $u(\alpha)$ are equal to $\mu=\Sigma_{i=1}^{3}\left(\frac{n_i}{\sqrt{i}}-2\pi\sqrt{2}\right)=0.933$ and $u(\alpha)=(0.933+\alpha)/\alpha^2$, respectively.

The peculiarity of dust plasma is that the charge Z is not an independent parameter, but decreases with increasing density of dust particles [see Eq. (9)].

Equations (52) and (9) define the dependence $U(N_d)$ in parametric form. The inclusion of the density dependence of charge brings about the emergence of a minimum for the potential curve and of a branch corresponding to the increase in potential with density. In what follows, the calculations are performed for fixed values of parameters typical of glow discharge: $T_e=2$ eV, $T_i=0.05$ eV, $N_i=10^8$ cm^{-3}, $a=5$ μm, and $M=1837*41$ (ionic mass of argon). For these values of parameters, the potential at the minimum for a liquidlike structure per particle is as high as $U_m=475$ eV, and the density of dust particles is $N_m=500$ cm^{-3}. Note that the energy at the minimum coincides in the order of magnitude with the energy of interaction of dust particles with $Z\sim 15\,000$ at an average distance $R\sim 0.07$ mm. Indeed, in this case $e^2Z^2/R\sim 440$ eV.

In what follows, it is convenient to introduce dimensionless units for energy and specific volume $U'=U/N_dU_m$ and $v=N_m/N_d$. The potential energies for liquid and crystal in these dimensionless variables are given in Fig. 6. These are typical curves for particle interaction with a minimum, with a steep branch corresponding to repulsion, and with a slowly decaying branch corresponding to attraction. As in the case of ordinary substances, the minimum of curve for crystal is deeper than that for liquid and is shifted towards smaller specific volumes.

X. DISCUSSION

The pressure decrease corresponding to potential (52) is obtained as a result of differentiation of energy with respect to volume $\Delta p = -\partial U/\partial V$. Because potential energy independent of the system volume makes no contribution to pressure, we have

$$\Delta p = -\frac{Z^2 e^2 N_d^{4/3}}{3 \times 2^{7/6}}\left(\mu + \frac{6N_d}{Z}\frac{\partial Z}{\partial N_d}(\mu+\alpha)\right). \quad (55)$$

The reduced pressures for liquid and crystal $\Delta p' = \Delta p/E_m N_m$, calculated from Eq. (55) for $\mu=0.933$ and 2.39, are given in Fig. 6. As it would be expected, the pressure goes to zero at the point of the minimum of potential.

To the negative pressure, we add the contribution of the thermal part in the Van der Waals form [14] to derive the equation of state for a highly correlated dust system,

$$p = \frac{N_d T}{1-4N_d V} - \frac{Z^2 e^2 N_d^{4/3}}{2^{7/6} \times 3}\left(\mu + \frac{6N_d}{Z}\frac{\partial Z}{\partial N_d}(\mu+\alpha)\right). \quad (56)$$

The quantity $4V$ in Eq. (53) corresponds to quadruplicate excluded volume. It is natural to take the particle volume fraction as this volume. In this case, $4V = 16\pi a^3/3 \sim 1.7 \times 10^{-10}$ cm^3. The dust concentration at the minimum of potential is $N_m = 500$ cm^{-3}; therefore, the correction $16\pi a^3 N_m/3 \sim 3 \times 10^{-6}$ is insignificant.

Let the temperature and concentration of dust particles be thermodynamic variables (the charge is a function of concentration). The rest of the parameters, which characterize the state of the plasma, remain constant. The question as to how this situation may be realized experimentally calls for special discussion. In this case, Eq. (56) may be used to estimate the critical point parameters. The regular procedure of determining the critical parameters, which consists of solving Eq. (56) along with conditions $dp/dN_d = d^2p/dN_d^2 = 0$, leads to the equations

$$-\frac{\partial \Delta p}{\partial N_d} 4VN_d = \frac{\partial^2 \Delta p}{\partial N_d^2}(1-4VN_d)N_d, \quad (57)$$

$$T_c = -\frac{\partial \Delta p}{\partial N_d}(1-4VN_d). \quad (58)$$

The first of these equations defines the critical density, and the second one—the critical temperature. Because $4VN_d \ll 1$, the critical density is determined by the inflection point of the density dependence of the potential part of pressure, i.e., from the condition $(\partial^2 \Delta p/\partial N_d^2)|_{Nd=Nc} = 0$. Then the critical temperature is found as $T_c = (\partial \Delta p/\partial N_d)|_{Nd=Nc} = 0$. Plotted in Fig. 7 are dimensionless isotherms of pressure according to Eq. (56) at $\mu=0.933$ (dust liquid). The temperature $T_c = 0.0675$ corresponds to the critical isotherm or, in dimensional units, $T_c \approx 34$ eV. The critical density is $N_c \approx 10$ or, in dimensional units, $N_c \approx 100$ cm^{-3}. The dimensionless pressure at the critical point is very low, $p_c \approx 0.001$. The charge of dust particles and the compressibility factor at the critical point are $Z_c \approx 18\,940$ and $\chi = p_c/T_c n_c \approx 0.23$. The isotherm at higher temperature is monotonic; at lower temperature, it has a minimum and a maximum. These critical parameters differ appreciably from those estimated in [16] using model pair potentials.

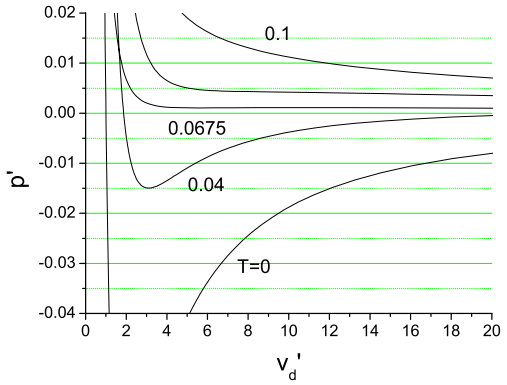

FIG. 7. (Color online) The isotherms according to Eq. (56) at different values of temperature. $T=0.0675$ correspond to the critical temperature.

The estimated critical parameters lead one to conclude that the critical mode may be realized for a very rarefied dust system, where the mean distance between dust particles may be equal to fractions of a centimeter, i.e., $\alpha \gg 1$. The positive potential at the boundary of Wigner-Seitz cell becomes very low and, consequently, the potential required for confinement of such plasma also becomes very low. However, it is difficult to observe the peculiarities in the critical behavior of dust plasma under laboratory conditions, because the confinement volume will contain too few dust particles. The situation becomes more favorable under microgravity conditions. In the majority of experiments, the dust temperature is lower than critical, and the density is much higher than critical. To draw an analogy with ordinary substances, one can maintain that the state of dust plasma under laboratory conditions corresponds to the subcritical solid, liquid, or amorphous states. In this case the liquid-solid phase transition is possible. This fact is confirmed by many experimental observations.

ACKNOWLEDGMENTS

This study was supported in part by the Program for Basic Research of the Presidium of the Russian Academy of Sciences on "Investigation of Matter under Extreme Conditions," by Max Planck Award Cooperation Research Program on Physics of High Energy Density Plasmas, by the Russian Foundation for Basic Research (Projects No. 06-02-17532, No. 05-02-17582a, No. 05-02-17607a, No. 05-08-33713a, and No. 06-03-32629a), and by NOW (Project No. 047.016.020).

[1] V. E. Fortov, A. G. Khrapak, S. A. Khrapak, V. I. Molotkov, and O. F. Petrov, Phys. Usp. **47**, 447 (2004).
[2] V. E. Fortov, A. V. Ievlev, S. A. Khrapak, A. G. Khrapak, and G. E. Morfill, Phys. Rep. **421**, 1 (2005).
[3] H. Thomas, G. E. Morfill, V. Demmel, J. Goree, B. Feuerbacher, and D. Mohlmann, Phys. Rev. Lett. **73**, 652 (1994).
[4] V. N. Tsytovich, Phys. Usp. **40**, 53 (1997).
[5] N. K. Ailawadi, Phys. Rep. **57**, 241 (1980).
[6] V. N. Tsytovich, J. Phys. A **39**, 1 (2006).
[7] S. A. Khrapak, A. V. Ivlev, G. E. Morfill, S. K. Zhdanov, and H. M. Thomas, IEEE Trans. Plasma Sci. **32**, 555 (2004).
[8] S. A. Khrapak, G. E. Morfill, A. G. Khrapak, and L. G. D'yachkov, Phys. Plasmas **13**, 052114 (2006).
[9] L. G. D'yachkov, A. G. Khrapak, S. A. Khrapak, and G. E. Morfill, Phys. Plasmas **14**, 042102 (2007).
[10] B. M. Smirnov, Phys. Usp. **44**, 1229 (2001).
[11] Ya. I. Frenkel, *Kineticheskaya teoriya zhidkostei (Kinetic Theory of Liquids)* (Nauka, Leningrad, 1975).
[12] Y. L. Al'pert, A. V. Gurevich, and L. P. Pitaevsky, *Space Physics with Artificial Satellites* (Consultants Bureau, New York, 1965).
[13] L. D. Landau and E. M. Lifshitz, *Statisticheskaya fizika (Statistical Physics)* (Nauka, Moscow, 1995).
[14] A. A. Likal'ter, Phys. Usp. **43**, 777 (2000).
[15] Ch. Kittel, *Introduction to Solid State Physics* (Wiley, New York, 1978).
[16] S. A. Khrapak, G. E. Morfill, A. V. Ivlev, H. M. Thomas, D. A. Beysens, B. Zappoli, V. E. Fortov, A. M. Lipaev, and V. I. Molotkov, Phys. Rev. Lett. **96**, 015001 (2006).